

See discussions, stats, and author profiles for this publication at: <https://www.researchgate.net/publication/5284950>

Probing the Active Center of Benzaldehyde Lyase with Substitutions and the Pseudosubstrate Analogue Benzoylphosphonic Acid Methyl Ester †

ARTICLE *in* BIOCHEMISTRY · AUGUST 2008

Impact Factor: 3.02 · DOI: 10.1021/bi8004413 · Source: PubMed

CITATIONS

19

READS

26

9 AUTHORS, INCLUDING:



[Sumit Chakraborty](#)

Cornell University

17 PUBLICATIONS 313 CITATIONS

[SEE PROFILE](#)



[Michael J Mcleish](#)

Indiana University-Purdue University Indiana...

105 PUBLICATIONS 1,809 CITATIONS

[SEE PROFILE](#)



[Gregory A. Petsko](#)

Brandeis University

485 PUBLICATIONS 25,608 CITATIONS

[SEE PROFILE](#)



[Frank Jordan](#)

Rutgers, The State University of New Jersey

288 PUBLICATIONS 6,083 CITATIONS

[SEE PROFILE](#)



NIH Public Access

Author Manuscript

Biochemistry. Author manuscript; available in PMC 2009 August 20.

Published in final edited form as:

Biochemistry. 2008 July 22; 47(29): 7734–7743. doi:10.1021/bi8004413.

Probing the active center of benzaldehyde lyase with substitutions and the pseudo-substrate analog benzoylphosphonic acid methyl ester

Gabriel S. Brandt[&], Natalia Nemeria[#], Sumit Chakraborty[#], Michael J. McLeish⁺, Alejandra Yep⁺, George L. Kenyon⁺, Gregory A. Petsko[&], Frank Jordan^{#, *, &}, and Dagmar Ringe^{*, &}

[&]Department of Biochemistry, Brandeis University, Waltham, MA 02454

[#]Department of Chemistry, Rutgers University, Newark, NJ 07102

⁺Department of Medicinal Chemistry, College of Pharmacy, University of Michigan, Ann Arbor, MI 48109.

Abstract

Benzaldehyde lyase (BAL) catalyzes the reversible cleavage of (*R*)-benzoin to benzaldehyde utilizing thiamin diphosphate and Mg²⁺ as cofactors. The enzyme is important for the chemoenzymatic synthesis of a wide range of compounds via its carboligation reaction mechanism. In addition to its principal functions, BAL can slowly decarboxylate aromatic amino acids such as benzoylformic acid. It is also intriguing mechanistically due to the paucity of acid-base residues at the active center that can participate in proton transfer steps thought to be necessary for these type of reactions. Here methyl benzoylphosphonate, an excellent electrostatic analog of benzoylformic acid, is used to probe the mechanism of benzaldehyde lyase. The structure of benzaldehyde lyase in its covalent complex with methyl benzoylphosphonate was determined to 2.49 Å (PDB ID: 3D7K) and represents the first structure of this enzyme with a compound bound in the active site. No large structural reorganization was detected compared to the complex of the enzyme with thiamin diphosphate. The configuration of the predecarboxylation thiamin-bound intermediate was clarified by the structure. Both spectroscopic and X-ray structural studies are consistent with inhibition resulting from the binding of MBP to the thiamin diphosphate in the active centers. We also delineated the role of His29 (the sole potential acid-base catalyst in the active site other than the highly conserved Glu50) and Trp163 in cofactor activation and catalysis by benzaldehyde lyase.

Benzaldehyde lyase (BAL; EC 4.1.2.38) is a thiamin diphosphate (ThDP)-dependent enzyme, which carries out the reversible conversion of (*R*)-benzoin to benzaldehyde (Eq 1). The enzyme is a valuable tool in chemoenzymatic synthesis of chiral α-hydroxyketones. (1,2) In addition to its lyase and carboligase activity, BAL is now clearly documented to have slow decarboxylase activity with benzoylformate, producing (*R*)-benzoin as a product and proceeding via the enamine intermediate (3). A plausible mechanism for the reactions carried out by BAL (Scheme 1) starts with a nucleophilic attack at the carbonyl carbon of benzoin by the ThDP ylide producing the first covalent intermediate C2-(α,β-dihydroxy-α,β-diphenyl)-ethylThDP (DDEThDP). DDEThDP releases the first molecule of benzaldehyde producing the enamine, which undergoes C2α-protonation to form C2α-hydroxybenzylThDP (HBThDP). A second molecule of benzaldehyde is then released and the ThDP ylide is regenerated (Scheme 1).

*To whom correspondence should be addressed: e-mail: ringe@brandeis.edu; tel: 781-736-4902; fax: 781-736-2405; frjordan@newark.rutgers.edu; tel: 973-353-5470; fax: 973-353-1264.

In the past, substrate analogs including sodium methyl acetylphosphonate, sodium acetylphosphinate and sodium acetyl methylphosphinate, have been found to be efficiently converted to the first covalent intermediate by a number of ThDP enzymes (4–7). By virtue of a C-P rather than C-C bond, this intermediate, an analog of C_{2α}-lactylthiamin diphosphate (LThDP), the pyruvate-ThDP adduct, is stable. Taking advantage of the decarboxylase activity found in BAL with benzoylformate, we have examined the interaction of this enzyme with benzoylphosphonic acid methyl ester (MBP, Figure 1). It was thought that MBP would behave as an analog of benzoylformate, onto which ThDP adds at the keto carbon in an enzyme-catalyzed reaction to form a C_{2α}-phosphonomandelylThDP methyl ester (PMThDP; Scheme 2). The latter is unable to undergo dephosphonylation, and would presumably form a stable pre-decarboxylation analog of C_{2α}-mandelylThDP (MThDP), the first covalent ThDP-bound intermediate in the decarboxylation of benzoylformate. In doing so, MBP might provide insight into the formation of intermediates with tetrahedral substitution at the C_{2α} atom, including the state of ionization and tautomeric nature of the 4'-aminopyrimidine ring of ThDP on BAL, a major current focus of research of the Rutgers group with several collaborators (4–6,8–12). We have now demonstrated in a number of ThDP-dependent enzymes that the 4'-aminopyrimidine ring of ThDP actively participates and plays a very crucial role in catalysis via its 1',4'-iminopyrimidine tautomeric form (4–7).

We show kinetically and spectroscopically that the stable intermediate indeed forms, and determine the structure of benzaldehyde lyase in its covalent complex with MBP to 2.49 Å (PDB ID: 3D7K). This represents the first structure of BAL with a substrate analog bound. No large structural reorganization was detected in this complex when compared to the complex of BAL with ThDP (13,14) or, as described below, to the complex of BAL with ThDP and sulfate.

The crystal structure of the BAL complexes reveals the presence of only two residues with side chains within 4 Å of the ThDP that are capable of proton transfer. The first is Glu50, a nearly universally conserved feature of thiamin enzymes, which is located within hydrogen bonding distance of the N1' atom of the 4'-aminopyrimidine ring, and it is presumed to participate in the acid-base chemistry leading to the 1',4'-iminopyrimidine tautomeric form of the coenzyme. The second is His29, which is hydrogen bonded to a water molecule 3.6 Å away from C2 of the thiazolium ring, but too far from the N4' atom to have any direct interaction with it.

Modeling of DDEThDP into the active site of BAL led to the suggestion that the side chain of His29 has a role in deprotonating the ‘distal’ OH group of the bound benzoin, triggering release of the first benzaldehyde molecule thus forming the enamine. Initial site-directed mutagenesis studies found that the H29A variant exhibited some reduction in activity, albeit apparently too small in magnitude for the residue to be participating in critical acid-base activity (15). We here further delineate the role of His29 and another active site residue, Trp163, in catalysis by BAL.

Materials and methods

Synthesis of methyl benzoylphosphonate

MBP was synthesized according to the method of Karaman, with some modifications (16). Briefly, dimethyl benzoylphosphonate was prepared by dropwise addition of 4.75 mL trimethylphosphite (5 g, 40.3 mmol) to 4.68 mL benzoyl chloride (5.66 g, 40.3 mmol) under nitrogen at 0 °C. After the addition was complete, the reaction mixture was stirred at 0 °C for 30 min and then allowed to warm to room temperature over a period of 3 h. The resulting yellowish oil was collected by vacuum distillation after a small forerun to yield 7.55 g (87%, lit. 89 %). ¹H NMR (500 MHz, CDCl₃, 0.5% TMS): δ 8.253 (d, J = 7.5 Hz, 2H), 7.652 (t, J = 7.5 Hz, 1H), 7.519 (t, J = 7.5 Hz, 2H), 3.922 (d, J = 10.5 Hz, 6H). A portion of the dimethyl benzoylphosphonate product (1 g, 4.67 mmol) was added to a solution of 2.1 g (14.01 mmol) of dry sodium iodide in 25 mL dry acetone under nitrogen, at 25 °C. After overnight stirring,

the reaction mixture was evaporated to dryness. The solid mixture was triturated several times with ethyl acetate and the solvent evaporated to dryness. The crude product was recrystallized from absolute ethanol to yield 0.82 g (79%, lit. 98%). ¹H NMR (500 MHz, D₂O-DSS): δ 8.202 (d, J = 7.5 Hz, 2H), 7.748 (t, J = 7.5 Hz, 1H), 7.612 (t, J = 7.5 Hz, 2H), 3.695 (d, J = 5.5 Hz, 3H).

Bacteria and plasmids

The plasmids pKKBAL-His, pKKBALH29A-His and pKKBALW163A-His were used for expression and purification of BAL and its H29A and W163A variants. The construction of H29A BAL was reported previously (15). For the construction of W163A BAL, site-directed mutagenesis was performed according to the QuikChange protocol using *Pfu* polymerase (Invitrogen) and pKKBAL-His (3) as a template. The forward primer used for mutagenesis is shown below with the mutated codon underlined and lowercase letters indicating a base change from wild type 5'- GTGTTGCTGGATCTGCCgcGGATATcCTGATGAACCAG-3'

The additional silent mutation was introduced to generate a new restriction site for EcoRV, which was used for the initial screening of the mutation by restriction analysis. The resulting plasmid was sequenced to ensure that only the intended mutation had occurred.

Expression and purification of BAL and its variants

The plasmid pKKBAL-His, pKKBALH29A-His and pKKBALW163A-His were transformed into BL21 (DE3)pLysS cells (Novagen). Expression and purification were carried out essentially as described (15). The fractions of highest purity as assessed by SDS-PAGE were pooled and the buffer was exchanged for the storage buffer (50 mM potassium phosphate buffer pH 6.5, 1 mM MgSO₄, 0.5 mM ThDP, 10% glycerol) using Econo-Pac 10 DG desalting columns (BioRad). The protein samples were concentrated with Amicon Ultra centrifugal filters (Millipore) and stored at -80 °C. The enzyme preparations were apparently homogeneous as judged by SDS-PAGE. Protein concentration was determined with the Bradford assay using bovine serum albumin as standard.

Activity and related measurements

The activity of BAL and its variants was measured in 1 mL of 50 mM Tris-HCl buffer (pH 8.0), containing 1 mg/mL of bovine serum albumin, 1 mM MgSO₄, 0.50 mM ThDP, 0.25 units of horse liver alcohol dehydrogenase (HLADH; 12.5 units/mL stock solution), 0.60 mM benzoin (0.01 M stock of benzoin was made in 99.9% DMSO) and 0.35 mM NADH. The reaction was initiated by the addition of 0.5 µg of BAL and was recorded for 5 min at 340 nm and 30 °C. The activity of BAL was approximately 30–40 units/mg protein.

Circular dichroism

CD studies were performed on a Chirascan CD Spectrometer from Applied Photophysics (Leatherhead, United Kingdom) in a 1 cm path length cell in the near UV region (as specified in each figure) at 30 °C unless otherwise specified. To the BAL (2 mg/mL, concentration of active centers =33.9 µM or as in the figure legends) in 50 mM Tris-HCl (pH 8.0) containing ThDP (150–200 µM) and MgSO₄ (1 mM), was added 1–500 µM MBP. To check for reversibility of inhibition by substrate analogs, the BAL titrated with substrate analog was dialyzed overnight against 2L of 50 mM Tris-HCl (pH 8.0) and the CD spectra were recorded.

Time-resolved CD

Stopped-flow circular dichroism experiments were carried out on a π*-180 CDF Spectrometer from Applied Photophysics using a slit width of 2 mm and a path length of 10 mm. The temperature was maintained at 30 °C. In a typical experiment, the required amount of BAL in

buffer A, containing 50 mM Tris-HCl (pH 8.0), 1 mM ThDP, 2.5 mM MgSO₄, 10% v/v DMSO (the DMSO is needed to keep the solutions homogeneous) was mixed with an equal volume of substrate of intended concentration in the same buffer. The reactions were monitored for varied time (0.01–200 s) and data points were collected at varied time interval (2.5–10 ms). The data were analyzed using Pro-K Global Analysis software. Single value decompositions (SVDs) were determined where necessary. SigmaPlot 2001 version 7.101 was used for all data analysis.

Protein crystallization

For co-crystallization of BAL with MBP, the procedure of Mosbacher *et al.* for wild-type BAL crystallization by vapor diffusion was followed closely (14). Briefly, BAL was dialyzed and then concentrated to 11 mg/mL (0.19 mM) in a solution of 5 mM HEPES (pH 6.9) also containing 10 mM NaCl, 2 mM MgCl₂, 2 mM DTT and 0.2 mM ThDP. Aliquots of the protein solution were flash-frozen in liquid nitrogen and stored at -80 °C. A well solution of 100 mM MES (pH 6.9) and 50% (v/v) PEG 200 was prepared. A stock solution of MBP was prepared at a concentration of 1 M in DMSO and likewise stored at -80 °C. In preparation for co-crystallization, the MBP solution was thawed and diluted 1:10 into the protein storage buffer. Typically, 0.2 µL MBP was incubated with 10 µL protein solution to give 10.8 mg/mL (0.19 mM) protein, 2 mM MBP and 0.2% v/v DMSO. Subsequent to this incubation, BAL-MBP solution was combined with well solution at a ratio of 1:1. The Mosbacher procedure makes use of a low-melting agarose solution as an additive (14). In our hands, no significant difference in crystallization rate, crystal appearance, or extent of diffraction was observed with the addition of agarose. Hundreds of small rod-like crystals typically appeared within 24 hours, many with a characteristic notch at each end. Larger crystals were typically obtained with the BAL-MBP complexes than with BAL alone, although the quality of diffraction was not significantly improved. Crystals were flash-frozen in liquid nitrogen without the use of additional cryoprotectant.

X-ray data collection

Crystals were irradiated at the beamline 19-ID administered by BioCARS (Advanced Photon Source, Argonne National Laboratory). Data reduction and processing were carried out using the HKL 2000 software package and the CCP4 suite of programs (17,18). A single monomer of the BAL crystal structure of Mosbacher (PDB code: 2AG0) was used as a search model for molecular replacement in Molrep (19) and Phaser (20). The unit cell of the BAL-MBP co-crystal was similar to that of BAL alone, but only half as long in its longest dimension. In order to obtain a molecular replacement solution, it was necessary to scale the data in the *P*3₂1 space group, the enantiomorph of the space group of BAL alone. The asymmetric unit was found to consist of a single dimer. Subsequent refinement of the data was carried out using the CCP4 software suite. Crystallographic data and refinement statistics are given in Table 1, and the PDB code of 3D7K has been assigned to the structure.

Structural refinement

Subsequent to molecular replacement, the initial model was refined using Refmac (21). Water molecules were added in an automated fashion into difference density peaks with an intensity greater than 3σ, using Coot software (22). Given the spatial resolution, the additional criteria of spherical shape, the presence of at least one hydrogen bonding partner, and location outside the active site were checked by hand and utilized in assigning water molecules to difference density (23,24). After refinement with a model including these water molecules, the ThDP cofactors were manually placed, using Coot, into the positive difference density and further positioned by real-space refinement. After refinement in the presence of polypeptide, water and cofactors, omit maps were generated and the ligand placed by an analogous process.

Coordinate files and appropriate restraints for the ThDP-MBP reaction product were generated using the Sketcher program of the CCP4 suite (25) and the PRODRG server (26). These restraints were retained for the ligand throughout refinement. After the cofactors and ligand were refined, active site waters were assigned to spherical regions of difference density greater than 4σ . A number of regions were observed to be disordered in the final structure and are indicated in Table 1. The final structural solution was subjected to validation using SFCheck, ProCheck and WhatCheck (27–29).

Results

MBP binds in the active center of benzaldehyde lyase

Kinetics of inhibition of BAL by MBP—We have shown previously that BAL can catalyze the decarboxylation of benzoylformate (3) and, given that methyl benzoyl phosphonate is an analog of benzoylformate, we thought MBP may also react with BAL. Preliminary experiments, carried out in the presence of 100 μ M benzoin (i.e., $\sim K_m$) showed that MBP had little effect until concentrations reached 1–2 mM whereupon some curvature was noticed in the progress curves (data not shown). This curvature was indicative of time-dependent inactivation, presumably due to the formation of C2 α -phosphonomandelylThDP (PMThDP). Accordingly we carried out a dilution study in which BAL (40 μ g/mL) was incubated with varying concentrations of MBP. At appropriate time intervals aliquots were assayed in the presence of saturating (*R*)-benzoin to determine the residual activity. The results, shown in Figure 1A, are clearly indicative of time- and concentration-dependent inhibition, but do not show evidence of saturation. A double-reciprocal (Kitz-Wilson) replot of the data from Figure 1A is presented in Figure 1B. The straight line with a y-intercept approaching zero suggests that only a weak complex is formed between BAL and MBP (30), and that the rate of inactivation is fast compared to the formation of the BAL.MBP complex. A plot of k_{obs} values against MBP concentration (not shown) yielded a second-order rate constant of 885 $M^{-1}min^{-1}$.

Circular dichroism observation of the 1',4'-iminopyrimidine form of a covalent intermediate on BAL using methyl benzoylphosphonate—Next, we needed to ascertain whether the covalent intermediate that MBP forms with ThDP resembles the pre-decarboxylation intermediate MThDP. This would be apparent from the CD band at 300–314 nm which reflects our general finding that ThDP analogs with tetrahedral substitution at the C2 α atom exist in their 1',4'-iminopyrimidine tautomeric form.

The near-UV CD spectrum (Figure 2) of BAL-ThDP displayed the negative CD band at 326 nm which has been assigned to the 4'-aminopyrimidine (AP) form of ThDP bound to the enzyme (5). On addition of 1–260 μ M MBP, this CD band was significantly reduced in amplitude and in its place a positive CD band at 312–314 nm developed and reached a limiting value ($S_{0.5}$ MBP = 25 μ M, Hill coefficient n_H = 2.0) (Figure 2). On the basis of model spectroscopic studies and CD studies on six ThDP enzymes (4–7,9,10,31), the CD band at 312–314 nm was assigned to the 1',4'-iminopyrimidine (IP) form of the first covalent intermediate on BAL, PMThDP (Scheme 2). The CD maximum for the IP form was shifted from 299 nm on BFDC (to be published) to 312–314 nm in BAL and this shift could be explained by the hydrophobic active centers of BAL, also supported by model studies at Rutgers (12).

The amplitude of the positive CD band at 314 nm was unchanged after overnight dialysis of a MBP-BAL complex. It was also shown that benzoin could regenerate activity when added to MBP-inhibited BAL, suggesting reversibility of MBP binding (data not shown). The reaction between BAL (2 mg/mL, concentration of active centers = 33.94 μ M) and 2 mM MBP was monitored by stopped-flow CD. A positive band at 313 nm developed and reached maximum

in approximately 10 s with a rate constant of $0.254 \pm 0.002 \text{ s}^{-1}$ for PMThDP formation (Figure 3).

The value of the Hill coefficient $n_H = 2.0$ (Figure 2 inset) indicates positive cooperativity of active centers on MBP binding (four active centers are suggested from X-ray structure). An $n_H = 1.42$ (with $S_{0.5} = 0.095 \text{ mM}$) was obtained from a steady-state kinetic experiment for (*R*)-benzoin breakdown to benzaldehyde, also indicating positive cooperativity of at least two active centers in BAL on substrate or substrate-analog binding (3). Size-exclusion chromatographic experiments suggested a molecular weight of 216 kDa, consistent with a tetramer in solution (32), as also suggested by the X-ray structure of BAL (14).

Structural characterization of BAL co-crystallized with MBP

In order to confirm the structure of the reaction product between enzyme and MBP, the structure of the complex was determined. BAL from *P. fluorescens* is a 555-amino acid polypeptide that is tetrameric in solution (32). In complex with methyl benzoylphosphonate, the protein crystallizes in the trigonal space group $P3_21$ with unit cell dimensions of $152 \times 152 \times 98 \text{ \AA}$. (Table 1) The asymmetric unit contains a dimer, rather than the dimer of dimers observed for the protein in the absence of MBP (13,14). A crystallographic two-fold axis recapitulates the tetrameric assembly seen in those structures. The substrate binding site is at the interface of the two subunits of the non-crystallographic dimer, and both binding sites are seen to be occupied in the crystal structure. Differences between the two binding sites represented in the asymmetric unit are slight, with 0.2 \AA RMSD among all sidechain atoms within 10 \AA of the ThDP cofactor. Binding of MBP does not cause large-scale structural rearrangements, as the structure superimposes readily on the previously reported structure of BAL (2AG0), with an overall alpha-carbon RMSD of 0.7 \AA and an all-atom RMSD of 0.4 \AA among sidechains within a 10 \AA radius of the cofactor. In co-crystallization experiments with MBP and BAL, an omit map indicated positive difference density contiguous with that of the cofactor. Chemically plausible alternate conformations and configurations (including both the *S*- and *R*-isomers, for example) of reacted and unreacted MBP were placed in the electron density, and the quality of fit was assessed by whether or not refinement of the model resulted in improved definition of the local electron density map. As shown in Figure 4, modeling the covalent adduct arising from addition of the thiazolium ylide to the carbonyl of MBP gave the best fit to the observed electron density.

Extrapolation from structural data—At a spatial resolution of 2.49 \AA , uncertainty about heavy atom positions makes assignment of hydrogen bonds somewhat equivocal (23,24). Likely hydrogen bonding interactions between the adduct and the protein that are supported by distance, geometry and chemical considerations are indicated in Figure 5. In addition, identification of water molecules is, to some extent, a matter of interpretation. Water molecules were placed in the active site only when omit maps of the active site show electron density with a clear signal ($> 4\sigma$). The methyl group of the MBP's monomethyl phosphonoester is not clearly evident in the electron density. This probably arises from heterogeneous distribution in active sites within the crystal. Since a definitive assignment may not be made, the methyl group is assigned at 1/3 occupancy to a single phosphonate oxygen.

MBP binding mode—The phosphonate group of MBP has only two potential hydrogen bonding partners, an active site water and the main chain amide nitrogen of Ala28 of the neighboring subunit (Figure 5). With respect to the carbinol oxygen resulting from thiazolium attack, both distance and geometry are consistent with an intramolecular hydrogen bond with the exocyclic imine ($N4'$) of the pyrimidinium ring of the cofactor and the amide nitrogen of Gln113. At this resolution, the orientation of the Gln sidechain is not fully resolvable, and the oxygen and nitrogen could be reversed. However, available experimental evidence favors the

assignment shown, as the CD spectrum confirms the identity of the 1',4'-imino form of the pyrimidinium ring. In this tautomer, the N4' lone pair is presented to the carbinol of MBP, fixing the directionality of the hydrogen bond. With regard to binding contacts between BAL and the phenyl ring of MBP, a pocket made up of the sidechains of Met 421A, Tyr 397A, Ala 394A, Ala 480A, Leu 398A and Leu 112B appears responsible, as each of these side chains approaches to within 5 Å of the phenyl atoms. (Figure 6)

BAL variants at His29 and Trp163

Kinetic consequences of the substitutions—On substitution of His29 or Trp163 with alanine, the activity measured in the presence of 0.50 mM ThDP was 2.7% (H29A) and 92% (W163A), respectively, compared to the activity of wild type BAL. (Figure 7–Figure 8) The absence of ThDP in the assay medium (in this case the ThDP was supplied by the enzyme only) did not affect the activity of wild-type (98%) or H29A (2.4%) but reduced the W163A BAL activity (56%), indicating that the W163A substitution affects ThDP binding, even though the X-ray structure shows that this residue is about 10 Å from the closest ThDP heavy atom and not directly involved in ThDP binding (Figure 10).

The rate of benzoin formed from benzaldehyde in the ligase reaction catalyzed by wild-type, H29A and W163A BAL was studied by stopped-flow CD. As shown in Figure 7, the reactions all displayed biphasic rate of formation of (*R*)-benzoin. In the fast phase, H29A was approximately 15 times slower ($1.15 \pm 0.57 \text{ s}^{-1}$; $0.37 \pm 0.01 \text{ s}^{-1}$) than wild-type ($16.2 \pm 1.85 \text{ s}^{-1}$; $0.62 \pm 0.03 \text{ s}^{-1}$), whereas W163A was almost two times slower ($7.84 \pm 0.53 \text{ s}^{-1}$; $0.46 \pm 0.02 \text{ s}^{-1}$). Conversely, in the slower phase, all variants displayed similar rates. Apparently, the H29A substitution affects both the lyase and ligase activities of BAL.

Circular dichroism observation of the interaction of ThDP with the H29A and W163A BAL variants—The CD spectra of the two BAL variants in the presence of 0.20 mM ThDP indicated the presence of the AP form of ThDP, as in the wild-type BAL. The amplitude of the negative CD band at 326 nm was 80% for W163A BAL compared to wild-type enzyme, while only a weak band was detected for H29A BAL (Figure 8A). Further, the CD spectrum of H29A BAL remained unchanged upon addition of 0.10–0.50 mM ThDP (data not shown). By contrast, with W163A BAL, the amplitude of the CD band at 326 nm increased on incremental addition of ThDP (Figure 8B), reaching a maximum ellipticity for a molar ratio of [ThDP]/[W163A subunits] = 16:1 as compared with the 1:1 ratio obtained for wild-type (not presented). Taken together, the data indicate that the W163A substitution on BAL affects ThDP binding. The H29A BAL shows much reduced amplitude for the AP form, perhaps due to a shift to the APH⁺ form of ThDP, a form which we can not detect by CD.

On addition of MBP, both the H29A and W163A variants developed the positive CD band at 312–314 nm that was seen with the wild type enzyme in Figure 2. The W163A BAL behaved similarly to wild type BAL ($S_{0.5, MBP} = 16.4 \mu\text{M}$, $n_H = 2.0$) (data not shown). With the H29A variant, while the intensity of the signal at 314 nm was only 27 % that of wild-type, its affinity for MBP was broadly similar ($S_{0.5, MBP} = 15.6 \mu\text{M}$, $n_H = 1.95$; Figure 9 inset).

Discussion

Mimicking the first reaction intermediate with the substrate analog MBP

The monomethyl ester of benzoyl phosphonate (MBP), an analog of the substrate benzoylformate, has been used in this study to provide insight into the first step of the benzaldehyde lyase reaction. The Kitz-Wilson plot (Figure 1B) shows the kinetics of inhibition by MBP, indicating that while bound in the active centers, MBP does not saturate the enzyme. The steady-state CD experiments (Figure 2) confirmed formation of the 1',4'-imino tautomer

of the covalent adduct between ThDP and MBP, and time-resolved CD experiments (Figure 3) determined the rate of adduct formation. Aliphatic congeners of MBP have been used as mechanism-based inhibitors of ThDP-dependent enzymes acting on pyruvate (4–7, 33–5). The products of these reactions are thought to be stable mimics for the complex that results from reaction between ThDP and pyruvate. The free acid, benzoylphosphonate, was found to inhibit the ThDP-dependent benzoylformate decarboxylase but, surprisingly, the inhibition resulted from phosphorylation of an active site serine rather than from formation of a stable adduct (36). The kinetic and CD spectroscopic evidence both suggest that MBP binds in the active centers of BAL and forms a covalent intermediate, C_{2α}-phosphonomandelylThDP, an analog of MThDP, the predecarboxylation intermediate derived from benzoylformate (Scheme 2). This was deduced from the positive CD band produced at 312–314 nm, which reflects the presence of the 1',4'-iminopyrimidine form of PMThDP. (Figure 2) This is characteristic of tetrahedral substitution at the C_{2α} atom of ThDP and has now been observed on six ThDP-dependent enzymes.

Crystal structure of covalent adduct of MBP

To attempt direct observation of the steady-state covalent complex, BAL was incubated with MBP and crystallized, following a published protocol for crystallization of native BAL (14). The structure was determined to a spatial resolution of 2.49 Å and represents the first reported structure of BAL with a substrate analog bound in the active site. (Table 1) The covalent nature of the adduct formed between MBP and the ThDP cofactor is clear from an examination of the active site electron density (Figure 4)

The first step of catalysis, which the cofactor-inhibitor complex in the present structure is thought to mimic, is not accompanied by any large-scale movements of either the BAL or the ThDP (RMSD 0.7 Å). Thus, our study confirms the prevailing notion that the enzyme positions the cofactor for catalysis prior to substrate binding (2,6,37–39). In this respect, BAL is similar to the other structurally characterized members of the family of ThDP-dependent enzymes. Indeed, comparison to pyruvate dehydrogenase (PDHc) and pyruvate oxidase (POX), both of which were recently characterized after irreversible inactivation with a phosphonate inhibitor, reveals very strong conservation of cofactor geometry (33,35).

Binding mode of MBP

Given that this is the first structure of a substrate analog in the BAL active site, some interpretation of the binding mode is warranted, in light of known mechanistic aspects of the reaction. Salient details of the binding are shown in Figure 5 and Figure 6. A fundamental mechanistic question is the identity of active site acids and bases responsible for proton transfer to and from the substrate. Surprisingly, the only credible candidate for general acid-base catalysis is His29. Thr481 of the second subunit is a conceivable proton donor, but its hydroxyl group is oriented away from the substrate in favor of a hydrogen-bonding opportunity with the backbone of Trp478. When a rotamer of Thr481 more favorable to substrate interaction was examined, refinement showed that fit of this alternate rotamer to the electron density was very poor. The closest approach of the ε nitrogen of His29 to a phosphate oxygen is 4.3 Å, implying that His29 would be too distant to have a direct acid-base interaction with the alcohol of BAL's benzoin substrate. However, we cannot rule out the possibility of structural rearrangement upon binding the natural substrate, benzoin, that would bring His29 within range.

Interaction with iminium N4' of ThDP

An interesting feature of thiamin-dependent catalysis is the potential for an intramolecular hydrogen bond to the carbinol oxygen formed by addition of the thiazolium ylide to the substrate carbonyl. Currently, data are available from the structures of pyruvate dehydrogenase (PDHc) and pyruvate oxidase (POX) (33,35). With acyl phosphonates, thiazolium attack

results in a methyl carbinol but, at the spatial resolution of these structures, the distinction between a methyl and hydroxyl group is not clear from the electron density. Therefore the assignment was made on chemical grounds. The lobe of electron density in position to make a hydrogen bond with the exocyclic amine of the ThDP pyrimidinium nitrogen was presumed to be the hydroxyl group (33,35). This assignment is undoubtedly reasonable, and evidence from the present structure would seem to confirm it. Addition to the benzoyl phosphonate results in a phenyl carbinol, and the hydroxyl and phenyl group are readily distinguished at a resolution of 2.49 Å. It is clear from this structure both that the depicted carbinol accounts more thoroughly for the observed omit map density than its enantiomer, and that the carbinol oxygen is well-positioned to make a hydrogen bond with ThDP. (Figure 4 and Figure 5) The importance of N4' to catalysis in ThDP-dependent enzymes is further emphasized by a recent study which suggests that oxidation of this functionality to the oxime abrogates activity in pyruvate-ferredoxin oxidoreductase (40).

The structure also permits analysis of how the enzyme enforces stereoelectronic constraints to influence the course of reaction (41). To explain the perpendicular alignment of the C-P bond with regard to the thiazolium ring, the hypothesis originally proposed by Dunathan may be invoked (42). The observed configuration aligns the C-C bond to be broken during decarboxylation with the π system of the thiazolium. In this way, the developing *p* orbital is geometrically disposed to achieve maximal overlap with the thiazolium π orbitals, thus lowering the barrier to bond breaking. This mechanism has been proposed for ThDP-dependent catalysis of decarboxylation (43–45). The present structure offers additional experimental corroboration of this model.

Effect of the H29A and W163A substitutions on ThDP binding, catalysis and tautomerization

In keeping with its position in the active site (Figure 5) and its possible role as an acid-base catalyst, the H29A variant had been shown to exhibit a tenfold reduction in value of k_{cat} although its K_m value for benzoin was largely unaffected (15). Trp163 is located above His29 and it could potentially be involved in a stacking interaction that could modulate the activity of His29. (Figure 10) In addition, it had been suggested that the negative CD band at 326 nm in other ThDP enzymes was the result of an interaction with Trp and the thiazolium ring of ThDP (46). To explore both these possibilities the H29A and W163A variants were prepared.

Confirming those of the early study (13), our results show that the H29A substitution decreases both the lyase and ligase activities of BAL. Conversely, the W163A substitution affects mostly the affinity of ThDP to BAL. The H29A substituted enzyme shows a very weak negative band at 326 nm in the near-UV CD spectra indicating one or both of the following: (a) the proper orientation of ThDP in the active center is affected, or (b) the pK_a for conversion of the APH⁺ to the AP form is shifted. In other words, if the pK_a increases, a smaller fraction of the AP form would be detected at the same pH (Scheme 1 left and ref 8 for this pK_a).

If His29 is indeed positively charged in the wild-type enzyme, this would tend to favor the AP form over the APH⁺ form. Now, conversion of His29 to Ala removes the positive charge, shifts the equilibrium to the APH⁺ (raising the pK_a compared to the wild-type), as evident from CD data, explaining: (a) a small band for the AP tautomer with ThDP; (b) a small band for the IP band with MBP and (c) lower activity in both lyase and ligase directions.

On addition of MBP both variants showed formation of the MBThDP covalent intermediate in its 1', 4'-iminopyrimidine tautomeric form. The W163A variant behaves similarly to wild type BAL but the H29A variant displays only a weak CD band in this region, again probably consistent with one of the explanations in the earlier paragraphs. Since Trp163 is distal to the ThDP binding site (~10 Å, Figure 10), it may be that both the activity and ThDP binding are affected by His29, raising the possibility of two distinct roles of His29. First, replacement of

His29 by alanine has a marked effect on the activity, confirming the importance suggested by its proximity to an important structural water molecule (Figure 5). Second, perhaps it plays a role in preventing ThDP from dissociating from the protein indirectly by its interaction with Trp163. It is tempting to speculate that the tryptophan side chain stacked, as it is, almost within van der Waals contact (3.5 Å) of His29 promotes protonation of the imidazole in the absence of substrate. Cation-pi interactions between tryptophan and imidazolium have been observed in numerous systems. (47–49).

If His29 is also too distant to interact with the substrate, why does its conversion to alanine have such a marked effect on activity? The present structure, like the structure of BAL without MBP bound, strongly suggests that His29 is critical in positioning the active site water rather than interacting directly with the substrate. More importantly, detailed analysis of the functional data shows that the substitution does not alter the enzyme's K_m value, but it does result in a roughly ten-fold decrease in k_{cat} (15). These data were interpreted to support the idea that proton transfer in the BAL active site is mediated by water. The present results showing that H29A substitution compromises the enzyme's ability to maintain the catalytically active cofactor tautomer may offer a different explanation for its effects on enzyme activity. However, short of unanticipated structural rearrangement, general acid-base catalysis is still the most plausible explanation for proton shuttling in the BAL active site.

Acknowledgments

Supported by NIH NRSA F32GM069057 (GSB, Brandeis), NIH GM050380 (Rutgers) and NSF EF-0425719 (Brandeis, Michigan).

Abbreviations used

ThDP, thiamin diphosphate
MThDP, C2 α -mandelylThDP, the covalent adduct formed between ThDP and benzoylformate
HBThDP, C2 α -hydroxybenzylThDP, the covalent adduct formed between ThDP and the product of the reaction benzaldehyde
LThDP, the covalent adduct formed between ThDP and pyruvate
BAL, benzaldehyde lyase
MBP, methyl benzoylphosphonate sodium salt
BFDC, benzoylformate decarboxylase
DDEThDP, C2-(α,β -dihydroxy- α,β -diphenyl)ethylThDP
PMThDP, C2 α -phosphonomandelyl thiamin diphosphate methyl ester
YPDC, pyruvate decarboxylase from the yeast *Saccharomyces cerevisiae*
POX, pyruvate oxidase from *Lactobacillus plantarum*
E1ec, the first component of the *Escherichia coli* pyruvate dehydrogenase complex
E1h, the first component of the human pyruvate dehydrogenase complex
SVD, single value decomposition
CD, circular dichroism
wt, wild type BAL

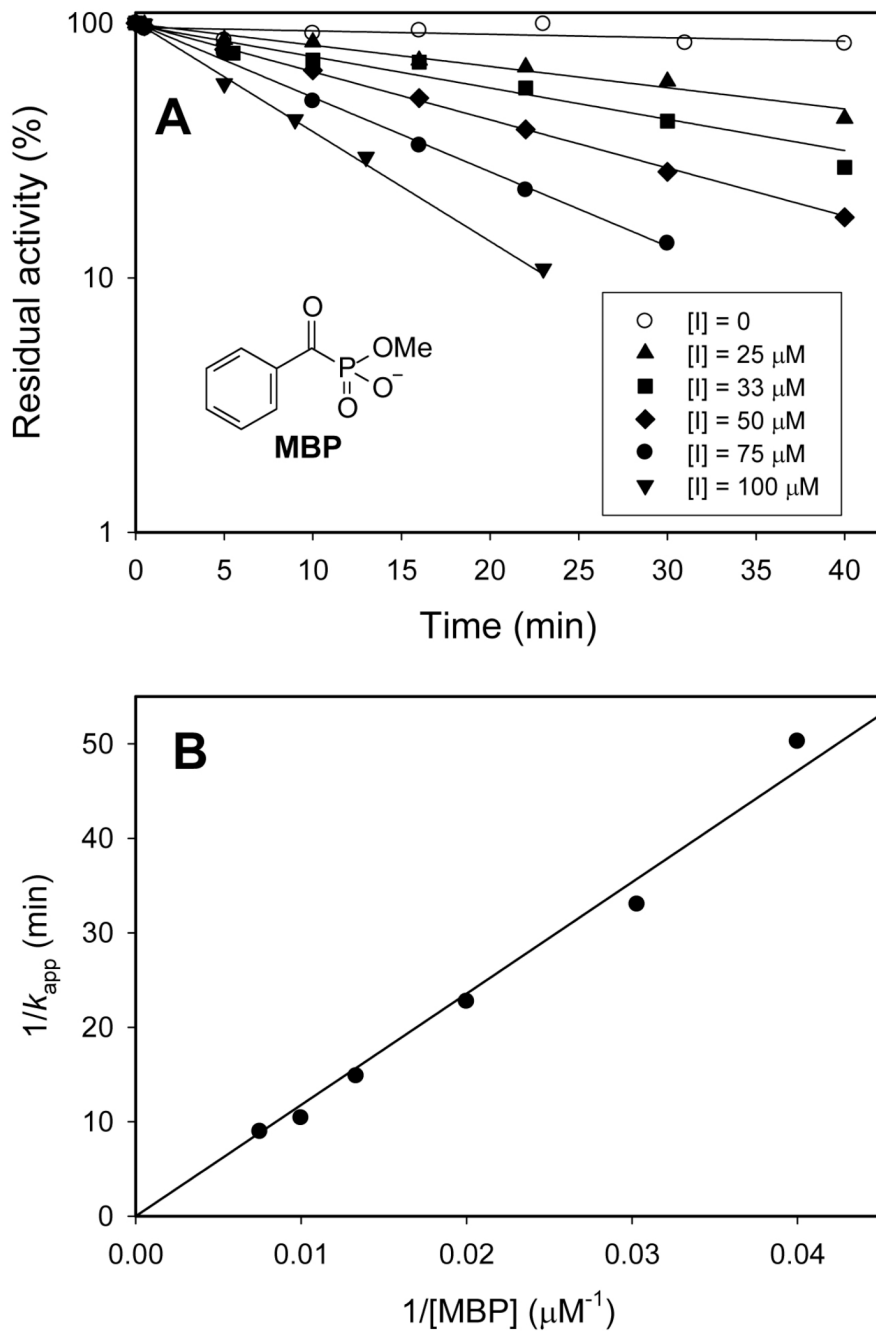
References

- Knoll M, Muller M, Pleiss J, Pohl M. Factors mediating activity, selectivity, and substrate specificity for the thiamin diphosphate-dependent enzymes benzaldehyde lyase and benzoylformate decarboxylase. *ChemBioChem* 2006;7:1928–1934. [PubMed: 17051662]
- Pohl M, Sprenger GA, Muller M. A new perspective on thiamine catalysis. *Curr. Opin. Biotechnol.* 2004;15:335–342. [PubMed: 15296931]

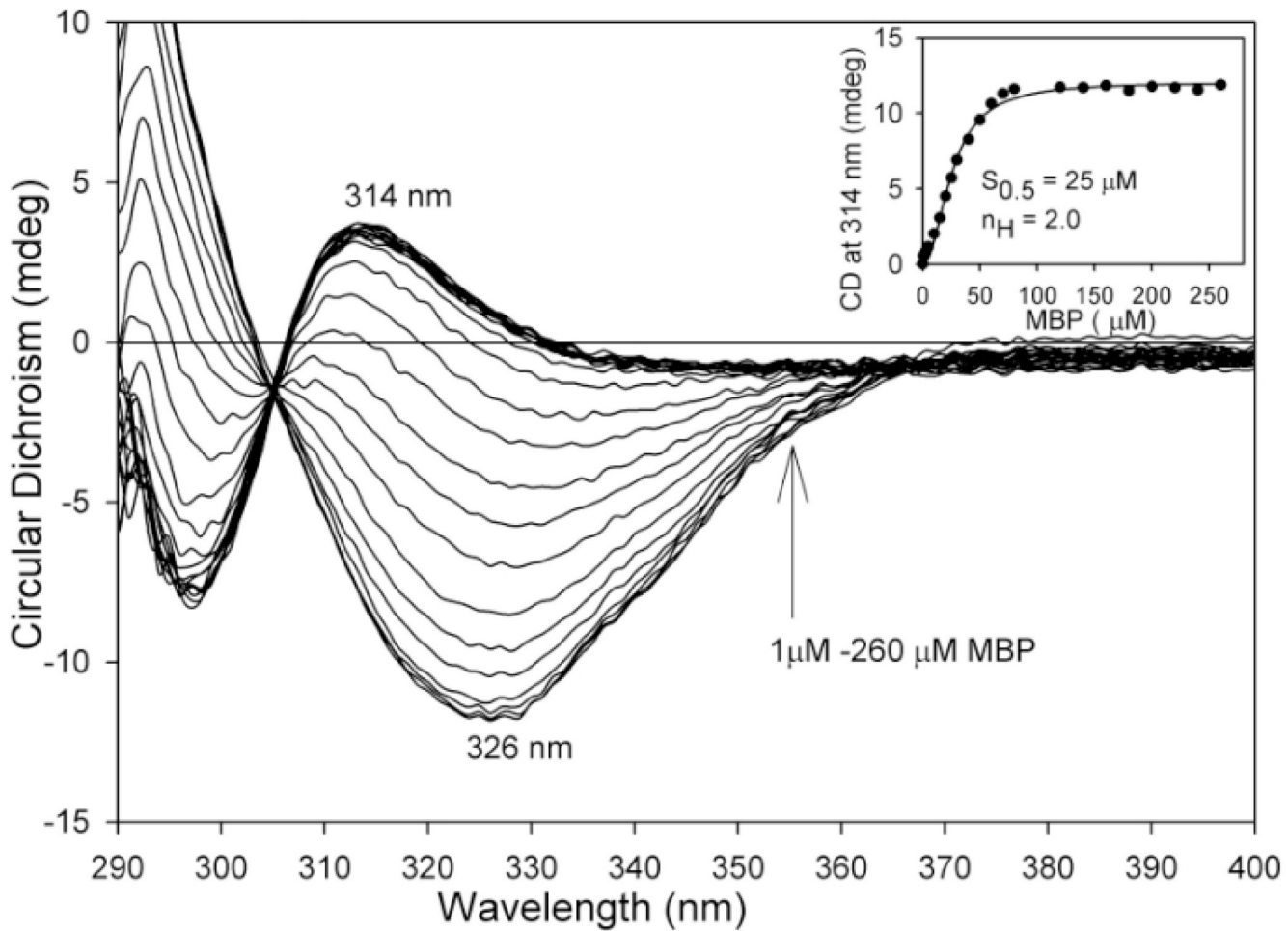
3. Chakraborty S, Nemeria N, Yep A, McLeish MJ, Kenyon GL, Jordan F. Mechanism of benzaldehyde lyase studied via thiamin diphosphate-bound intermediates and kinetic isotope effects. *Biochemistry*. 2008;in press.
4. Nemeria N, Baykal A, Joseph E, Zhang S, Yan Y, Furey W, Jordan F. Tetrahedral intermediates in thiamin diphosphate-dependent decarboxylations exist as a 1',4'-imino tautomeric form of the coenzyme, unlike the Michaelis complex or the free coenzyme. *Biochemistry* 2004;43:6565–6575. [PubMed: 15157089]
5. Nemeria N, Korotchkina L, McLeish MJ, Kenyon GL, Patel MS, Jordan F. Elucidation of the chemistry of enzyme-bound thiamin diphosphate prior to substrate binding: defining internal equilibria among tautomeric and ionization states. *Biochemistry* 2007;46:10739–10744. [PubMed: 17715948]
6. Jordan F. Current mechanistic understanding of thiamin diphosphate-dependent enzymatic reactions. *Nat. Prod. Rep.* 2003;20:184–201. [PubMed: 12735696]
7. Nemeria N, Chakraborty S, Baykal A, Korotchkina LG, Patel MS, Jordan F. The 1',4'-iminopyrimidine tautomer of thiamin diphosphate is poised for catalysis in asymmetric active centers on enzymes. *Proc. Natl Acad. Sci. USA* 2007;104:78–82. [PubMed: 17182735]
8. Jordan F, Mariam YH. N1'-methylthiaminium diiodide - model study on effect of a coenzyme bound positive charge on reaction-mechanisms requiring thiamin pyrophosphate. *J. Am. Chem. Soc.* 1978;100:2534–2541.
9. Jordan F, Zhang Z, Sergienko E. Spectroscopic evidence for participation of the 1',4'-imino tautomer of thiamin diphosphate in catalysis by yeast pyruvate decarboxylase. *Bioorganic Chemistry* 2002;30:188–198. [PubMed: 12406703]
10. Nemeria N, Tittmann K, Joseph E, Zhou L, Vazquez-Coll MB, Arjunan P, Hubner G, Furey W, Jordan F. Glutamate 636 of the *Escherichia coli* pyruvate dehydrogenase-E1 participates in active center communication and behaves as an engineered acetolactate synthase with unusual stereoselectivity. *J. Biol. Chem.* 2005;280:21473–21482. [PubMed: 15802265]
11. Schellenberger A. Sixty years of thiamin diphosphate biochemistry. *Biochim. Biophys. Acta-Protein Struct. Molec. Enzym.* 1998;1385:177–186.
12. Baykal AT, Kakalis L, Jordan F. Electronic and nuclear magnetic resonance spectroscopic features of the 1',4'-iminopyrimidine tautomeric form of thiamin diphosphate, a novel intermediate on enzymes requiring this coenzyme. *Biochemistry* 2006;45:7522–7528. [PubMed: 16768448]
13. Maraite A, Schmidt T, Ansorge-Schumacher MB, Brzozowski AM, Grogan G. Structure of the ThDP-dependent enzyme benzaldehyde lyase refined to 1.65 Å resolution. *Acta Cryst. D-Biol. Cryst.* 2007;63:546–548.
14. Mosbacher TG, Mueller M, Schulz GE. Structure and mechanism of the ThDP-dependent benzaldehyde lyase from *Pseudomonas fluorescens*. *FEBS J* 2005;272:6067–6076. [PubMed: 16302970]
15. Kneen MM, Pogozheva ID, Kenyon GL, McLeish MJ. Exploring the active site of benzaldehyde lyase by modeling and mutagenesis. *Biochim. Biophys. Acta* 2005;1753:263–271. [PubMed: 16226928]
16. Karaman R, Goldblum A, Breuer E, Leader H. Acylphosphonic acids and methyl hydrogen acylphosphonates - physical and chemical properties and theoretical calculations. *J. Chem. Soc.-Perkin Trans* 1989;1:765–774.
17. Bailey S. The CCP4 suite - programs for protein crystallography. *Acta Cryst. D-Biol. Cryst.* 1994;50:760–763.
18. Otwinski Z, Minor W. Processing of X-ray diffraction data collected in oscillation mode. *Meth. Enz.* 1997;276:307–326.
19. Vagin A, Teplyakov A. MOLREP: an automated program for molecular replacement. *J. Appl. Cryst.* 1997;30:1022–1025.
20. McCoy AJ, Grosse-Kunstleve RW, Adams PD, Winn MD, Storoni LC, Read RJ. Phaser crystallographic software. *J. Appl. Cryst.* 2007;40:658–674. [PubMed: 19461840]
21. Murshudov GN, Vagin AA, Dodson EJ. Refinement of macromolecular structures by the maximum-likelihood method. *Acta Cryst. D-Biol. Cryst.* 1997;53:240–255.
22. Emsley P, Cowtan K. Coot: model-building tools for molecular graphics. *Acta Cryst. D-Biol. Cryst.* 2004;60:2126–2132.

23. Acharya KR, Lloyd MD. The advantages and limitations of protein crystal structures. *Trends Pharmacol. Sci* 2005;26:10–14. [PubMed: 15629199]
24. Kleywegt GJ. Validation of protein crystal structures. *Acta Cryst. D-Biol. Cryst* 2000;56:249–265.
25. Potterton E, Briggs P, Turkenburg M, Dodson E. A graphical user interface to the CCP4 program suite. *Acta Cryst. D-Biol. Cryst* 2003;59:1131–1137.
26. Schuttelkopf AW, van Aalten DMF. PRODRG: a tool for high-throughput crystallography of protein-ligand complexes. *Acta Cryst. D-Biol. Cryst* 2004;60:1355–1363.
27. Hooft RW, Vriend G, Sander C, Abola EE. Errors in protein structures. *Nature* 1996;381:272. [PubMed: 8692262]
28. Laskowski RA, MacArthur MW, Moss DS, Thornton JM. PROCHECK - a program to check the stereochemical quality of protein structures. *J. Appl. Cryst* 1993;26:283–291.
29. Vaguine AA, Richelle J, Wodak SJ. SFCHECK: a unified set of procedures for evaluating the quality of macromolecular structure-factor data and their agreement with the atomic model. *Acta Cryst. D-Biol. Cryst* 1999;55:191–205.
30. Kitz R, Wilson IB. Esters of methanesulfonic acid as irreversible inhibitors of acetylcholinesterase. *J. Biol. Chem* 1962;237:3245–3249. [PubMed: 14033211]
31. Baykal A, Chakraborty S, Dodoor A, Jordan F. Synthesis with good enantiomeric excess of both enantiomers of alpha-ketols and acetolactates by two thiamin diphosphate-dependent decarboxylases. *Bioorganic Chemistry* 2006;34:380–393. [PubMed: 17083961]
32. Janzen E, Muller M, Kolter-Jung D, Kneen MM, McLeish MJ, Pohl M. Characterization of benzaldehyde lyase from *Pseudomonas fluorescens*: A versatile enzyme for asymmetric C-C bond formation. *Bioorganic Chemistry* 2006;34:345–361. [PubMed: 17078994]
33. Arjunan P, Sax M, Brunskill A, Chandrasekhar K, Nemeria N, Zhang S, Jordan F, Furey W. A thiamin-bound, pre-decarboxylation reaction intermediate analogue in the pyruvate dehydrogenase E1 subunit induces large scale disorder-to-order transformations in the enzyme and reveals novel structural features in the covalently bound adduct. *J. Biol. Chem* 2006;281:15296–15303. [PubMed: 16531404]
34. Jordan F, Nemeria NS. Experimental observation of thiamin diphosphate-bound intermediates on enzymes and mechanistic information derived from these observations. *Bioorganic Chemistry* 2005;33:190–215. [PubMed: 15888311]
35. Wille G, Meyer D, Steinmetz A, Hinze E, Golbik R, Tittmann K. The catalytic cycle of a thiamin diphosphate enzyme examined by cryocrystallography. *Nature Chemical Biology* 2006;2:324–328.
36. Bera AK, Polovnikova LS, Roestamadji J, Widlanski TS, Kenyon GL, McLeish MJ, Hasson MS. Mechanism-based inactivation of benzoylformate decarboxylase, a thiamin diphosphate-dependent enzyme. *J. Am. Chem. Soc* 2007;129:4120–4121. [PubMed: 17367138]
37. Frank RAW, Leeper FJ, Luisi BF. Structure, mechanism and catalytic duality of thiamine-dependent enzymes. *Cell. Mol. Life Sci* 2007;64:892–905. [PubMed: 17429582]
38. Lie MA, Celik L, Jorgensen KA, Schiott B. Cofactor activation and substrate binding in pyruvate decarboxylase. Insights into the reaction mechanism from molecular dynamics simulations. *Biochemistry* 2005;44:14792–14806. [PubMed: 16274227]
39. Malandrinos G, Louloudi M, Hadjiliadis N. Thiamine models and perspectives on the mechanism of action of thiamine-dependent enzymes. *Chem. Soc. Rev* 2006;35:684–692. [PubMed: 16862269]
40. Cavazza C, Contreras-Martel C, Pieulle L, Chabriere E, Hatchikian EC, Fontecilla-Camps JC. Flexibility of thiamine diphosphate revealed by kinetic crystallographic studies of the reaction of pyruvate-ferredoxin oxidoreductase with pyruvate. *Structure* 2006;14:217–224. [PubMed: 16472741]
41. Eliot AC, Kirsch JF. Avoiding the road less traveled: How the topology of enzyme-substrate complexes can dictate product selection. *Acc. Chem. Res* 2003;36:757–765. [PubMed: 14567709]
42. Dunathan HC. Conformation and reaction specificity in pyridoxal phosphate enzymes. *Proc. Natl Acad. Sci. USA* 1966;55:712–716. [PubMed: 5219675]
43. Hoskins AA, Moran M, Kappock TJ, Mathews II, Zaugg JB, Bader TE, Peng P, Okamoto A, Ealick SE, Stubbe J. N-5-CAIR mutase: Role of a CO₂ binding site and substrate movement in catalysis. *Biochemistry* 2007;46:2842–2855. [PubMed: 17298082]

44. Hu Q, Kluger R. Fragmentation of the conjugate base of 2-(1-hydroxybenzyl)thiamin: does benzoylformate decarboxylase prevent orbital overlap to avoid it? *J. Am. Chem. Soc* 2004;126:68–69. [PubMed: 14709063]
45. Wang JY, Dong H, Li SH, He HW. Theoretical study toward understanding the catalytic mechanism of pyruvate decarboxylase. *J. Phys. Chem. B* 2005;109:18664–18672. [PubMed: 16853401]
46. Kochetov GA, Usmanov RA. Charge transfer interactions in transketolase-thiamine pyrophosphate complex. *Biochem. Biophys. Res. Comm* 1970;41:1134–1140. [PubMed: 5483618]
47. Fernandez-Recio J, Vazquez A, Civera C, Sevilla P, Sancho J. The tryptophan/histidine interaction in alpha-helices. *J. Mol. Bio* 1997;267:184–197. [PubMed: 9096217]
48. Okada A, Miura T, Takeuchi H. Protonation of histidine and histidine-tryptophan interaction in the activation of the M2 ion channel from influenza a virus. *Biochemistry* 2001;40:6053–6060. [PubMed: 11352741]
49. Takeuchi H, Okada A, Miura T. Roles of the histidine and tryptophan side chains in the M2 proton channel from influenza A virus. *FEBS Lett* 2003;552:35–38. [PubMed: 12972149]

**Figure 1.**

(Top) Time- and concentration-dependent inactivation of BAL by MBP. The structure of MBP is inset. (Bottom) Reciprocal (Kitz and Wilson) plot of $1/k_{\text{inact}}$, observed versus $1/\text{[MBP]}$. BAL (40 $\mu\text{g/mL}$, 0.68 μM active centers) in 50 mM Tris-HCl (pH 8.0) containing 1 mM MgSO_4 and 0.5 mM ThDP was incubated with MBP (25–100 μM) at 30 °C. At appropriate time intervals aliquots (10 μL) were withdrawn and diluted 1:100 into a standard assay mixture containing 1 mM benzoin.

**Figure 2.**

Near-UV CD spectra of BAL treated with MBP (inset). BAL (2.5 mg/ml, concentration of active centers = 41.67 μM) in 50 mM Tris-HCl (pH 8.0) containing 1 mM ThDP and 2.5 mM MgSO₄ was titrated with MBP (1–260 μM). Inset shows that the positive CD band at 314 nm reached the limiting value with K_{d, MBP} = 25 μM and n_H = 2.0. The CD at 314 nm was obtained by the subtraction of the CD at 314 nm in the absence of MBP.

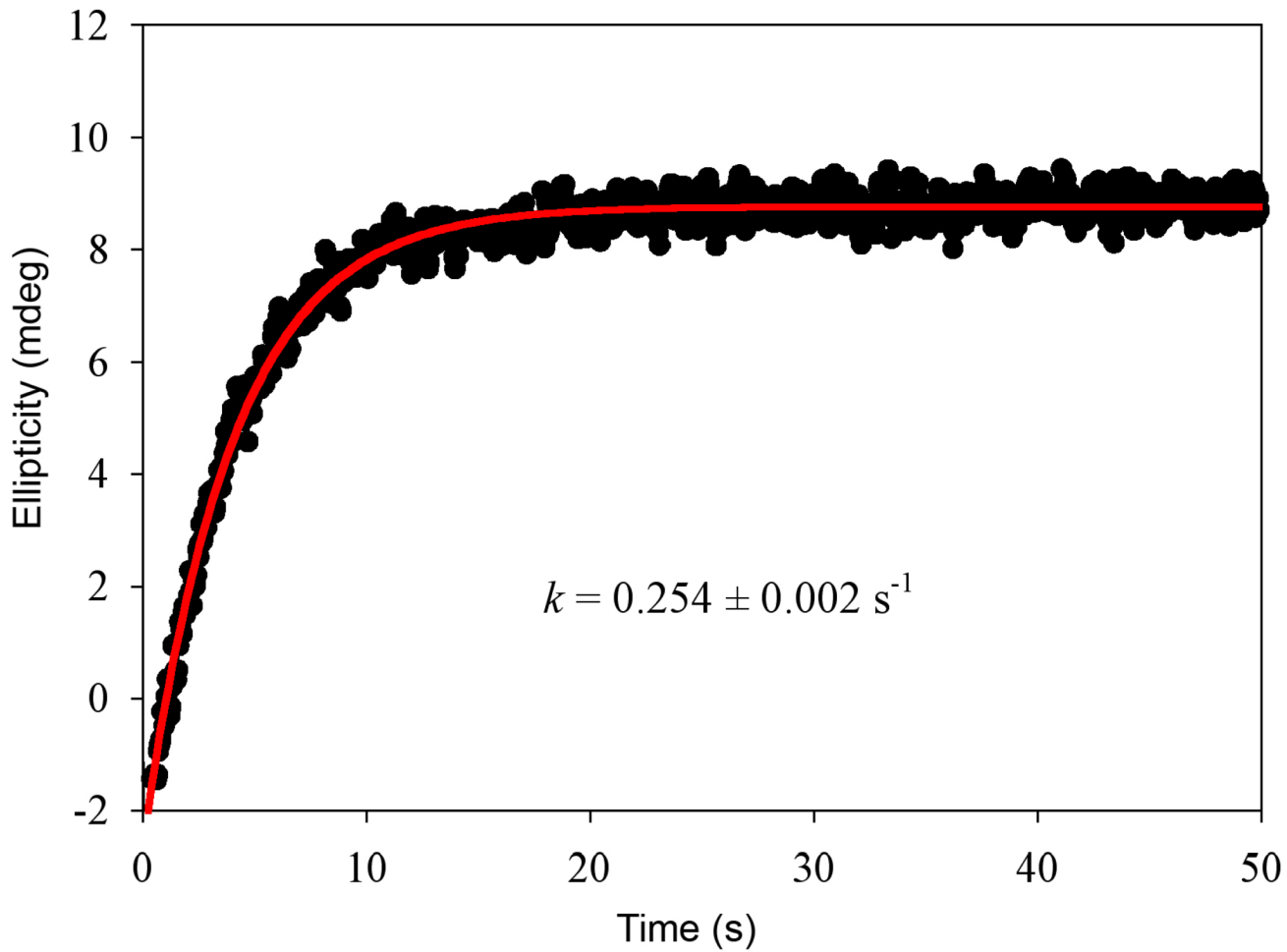


Figure 3.

Rate of 1', 4'-imino-PMThDP formation from MBP by BAL using stopped-flow CD. BAL (2.0 mg/ml, concentration of active centers = 33.9 μM) in 50 mM Tris-HCl (pH 8.0), containing 1 mM ThDP, 2.5 mM MgSO₄ and 10% (v/v) DMSO in one syringe was mixed with equal volume of 1 mM MBP in the same buffer in the second syringe and the reaction was monitored at 313 nm for 50s at 30 °C as presented under Experimental Procedures. Data were fitted to a single exponential rise to maximum.

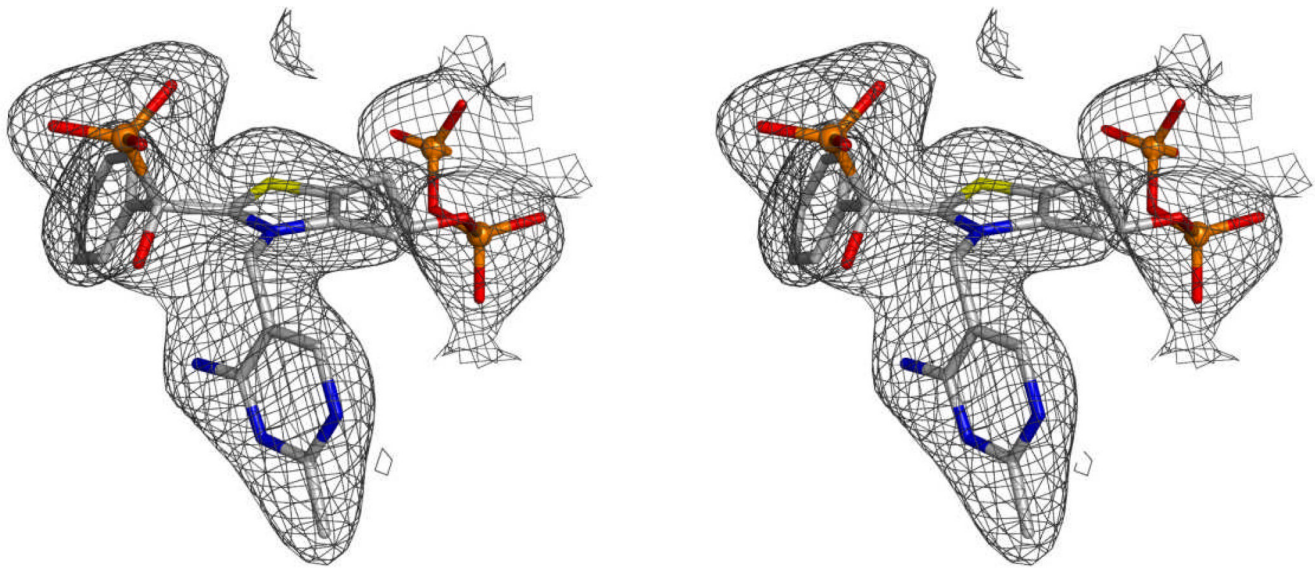
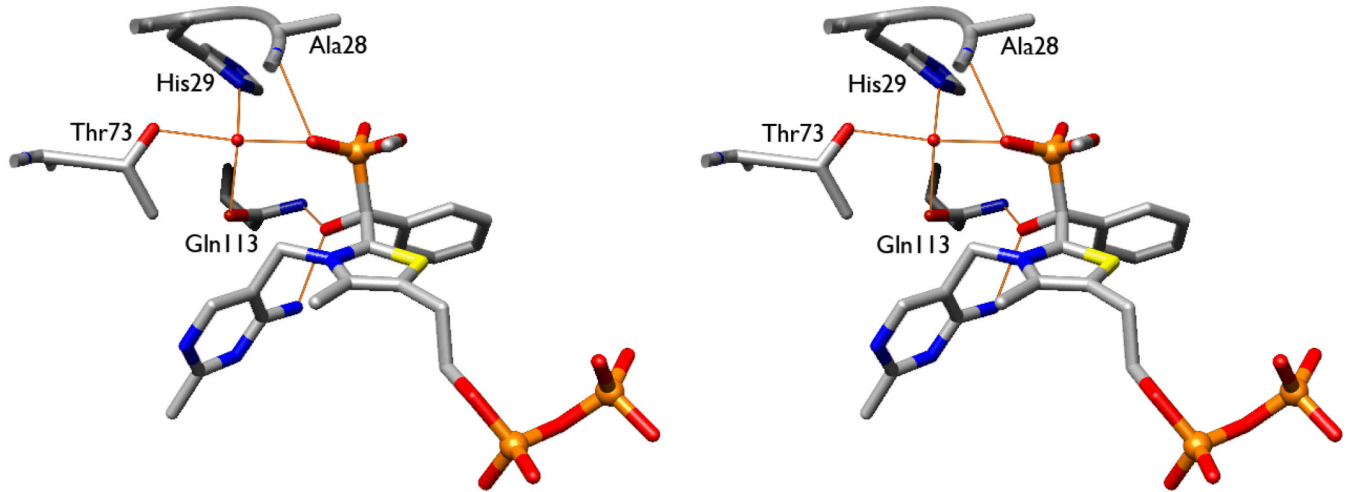


Figure 4.

Stereo view of the covalent adduct formed between the ThDP cofactor of BAL and the inhibitor MBP, showing the newly formed covalent bond to MBP. Grey mesh represents an electron density map with coefficients $2F_O - F_C$ contoured at 1σ . For clarity, the methyl group of the MBP phosphonester is not shown. (PDB ID: 3D7K)

**Figure 5.**

Stereo view of the BAL ThDP-MBP adduct, showing the probable hydrogen bonding network of MBP.

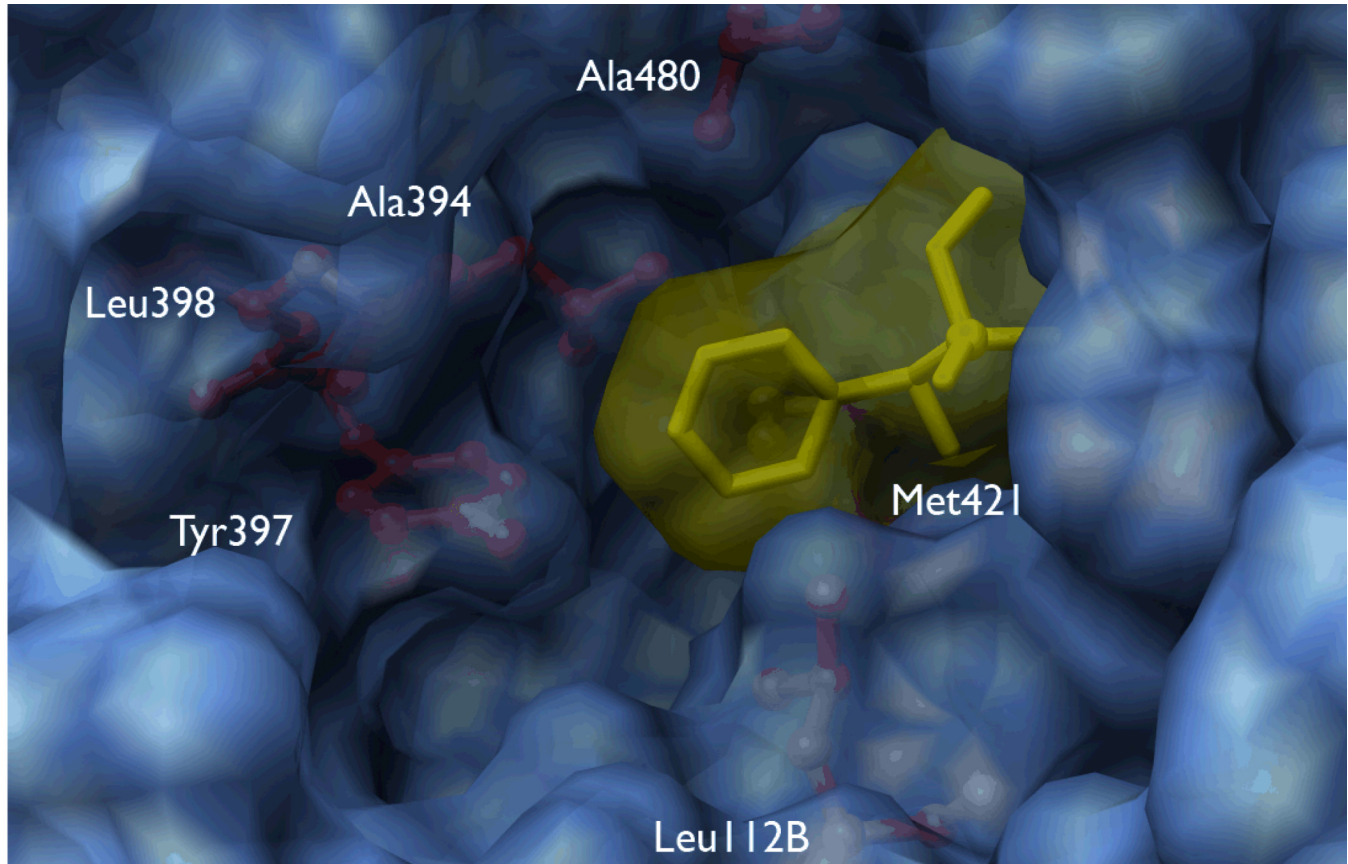


Figure 6.

Surface rendering of BAL with bound MBP, showing the residues (red) making up the hydrophobic binding pocket for the phenyl ring of the inhibitor (yellow). For clarity, the ThDP cofactor is not shown.

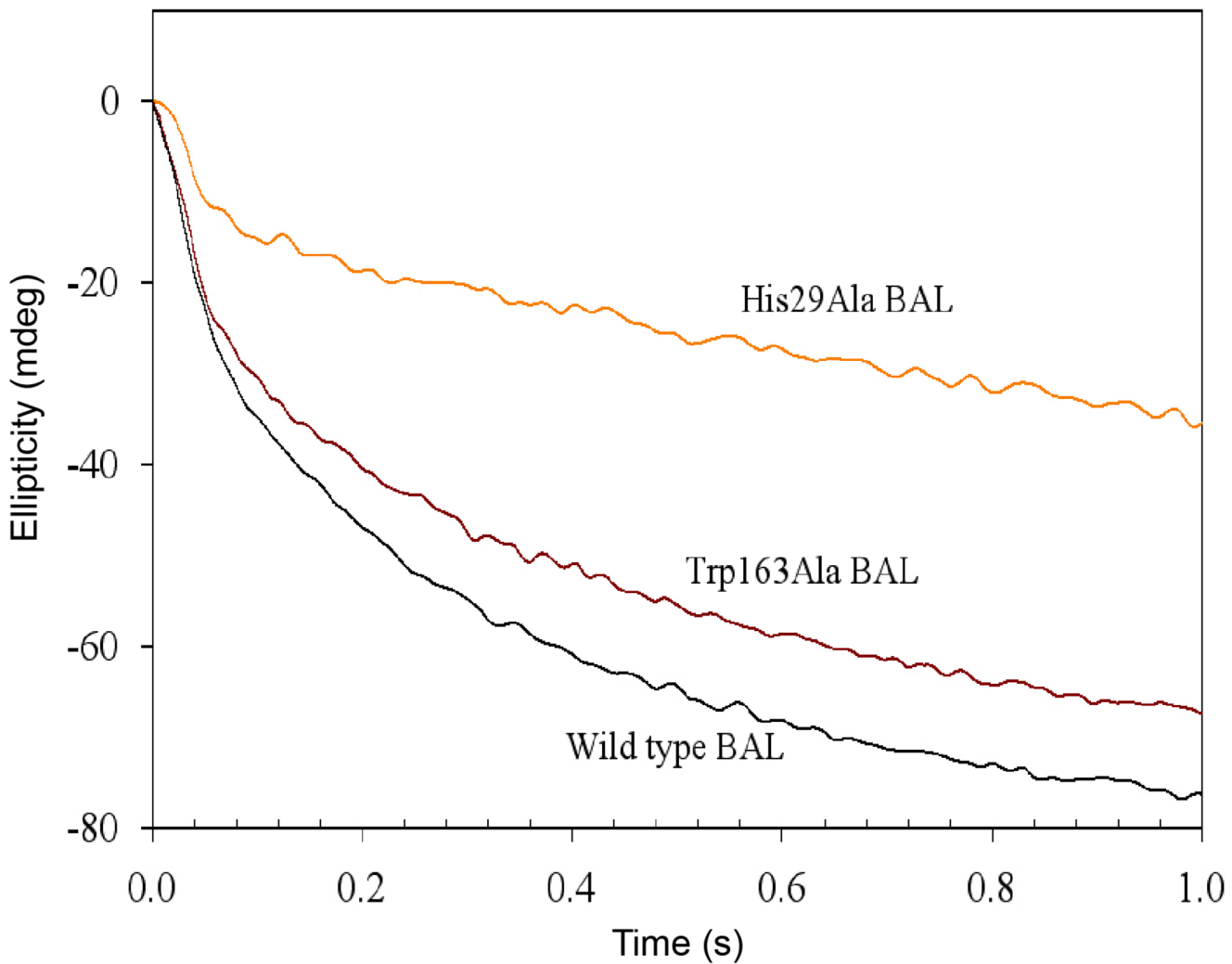
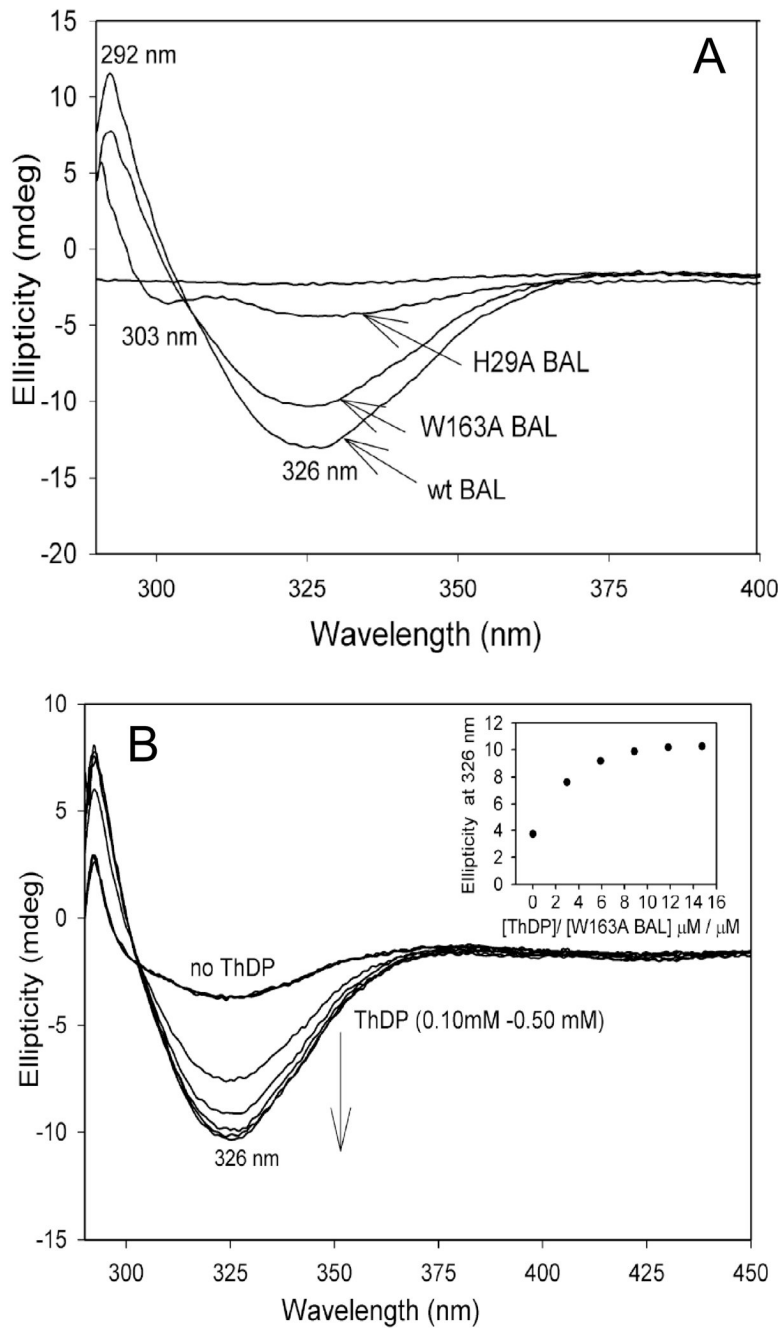
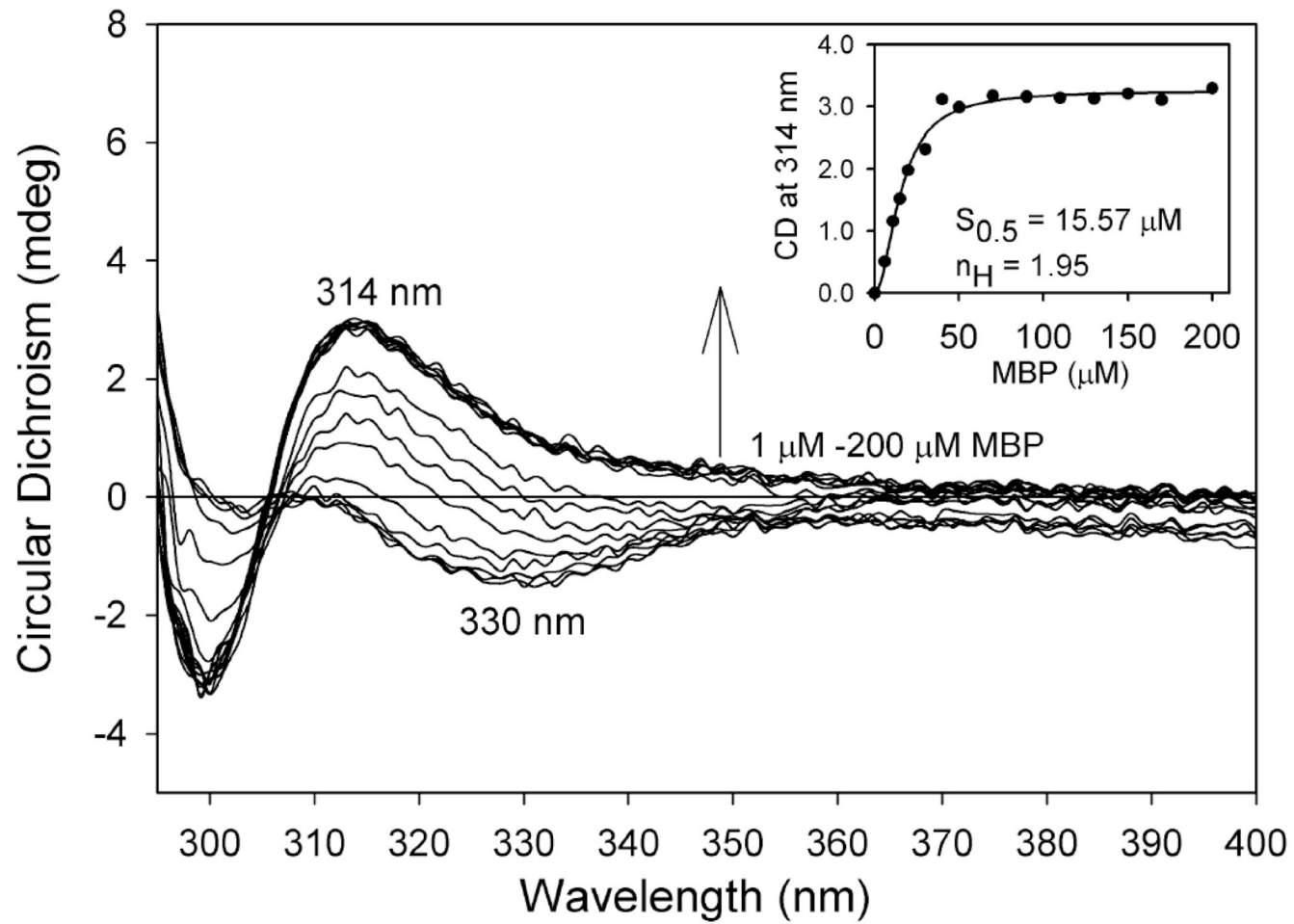


Figure 7.

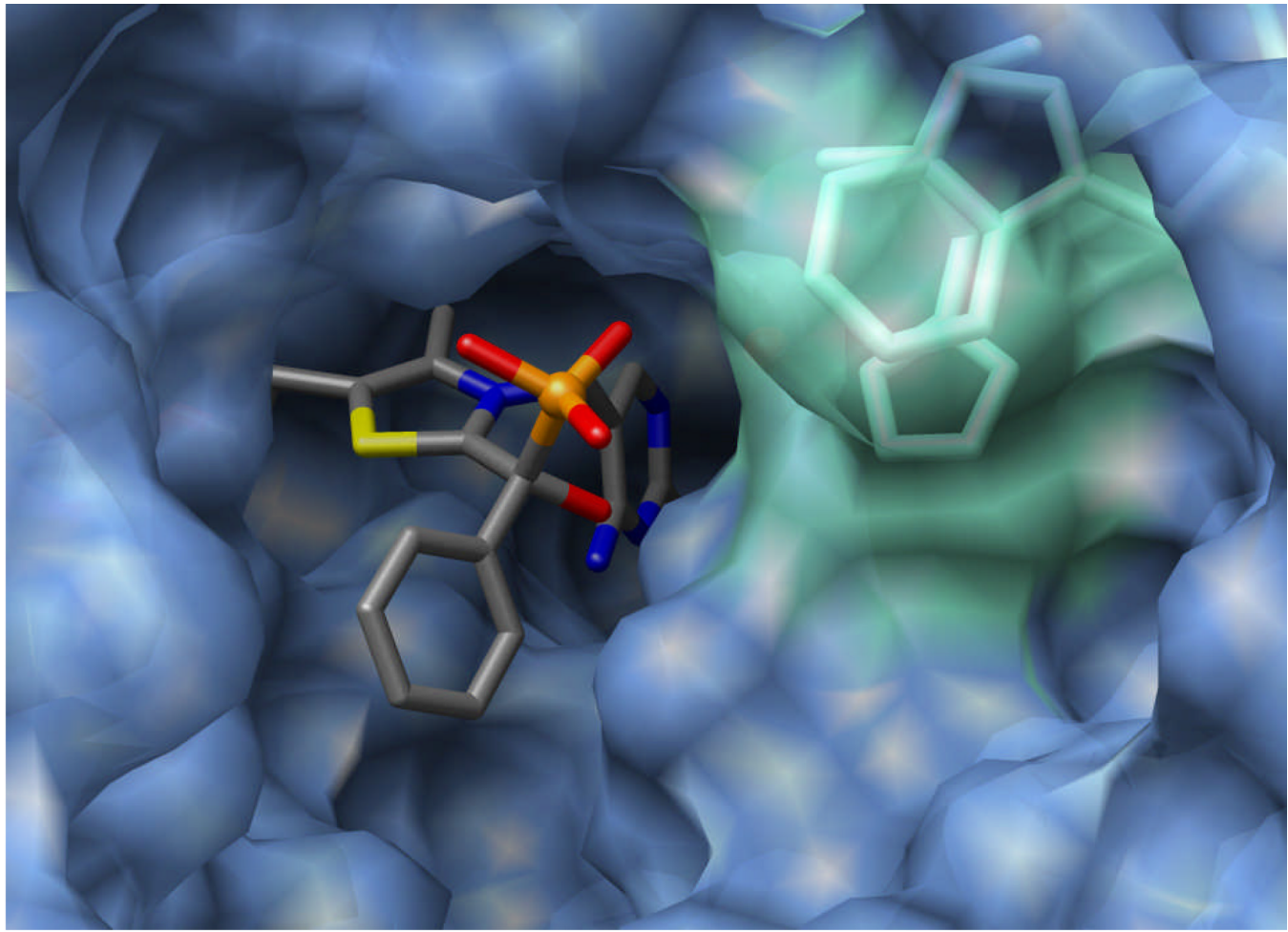
Detection of (*R*)-benzoin formation in stopped-flow CD. BAL (2 mg/mL, 33.94 μ M) in 50 mM Tris-HCl (pH 8.0), containing 1 mM MgSO₄ and 0.20 mM ThDP was mixed with an equal volume of 20 mM benzaldehyde in the same buffer. The reaction was monitored at 313 nm in a 10 mm cell with 2 nm slit width for 5 s. Data points were collected every 2.5 ms.

**Figure 8.**

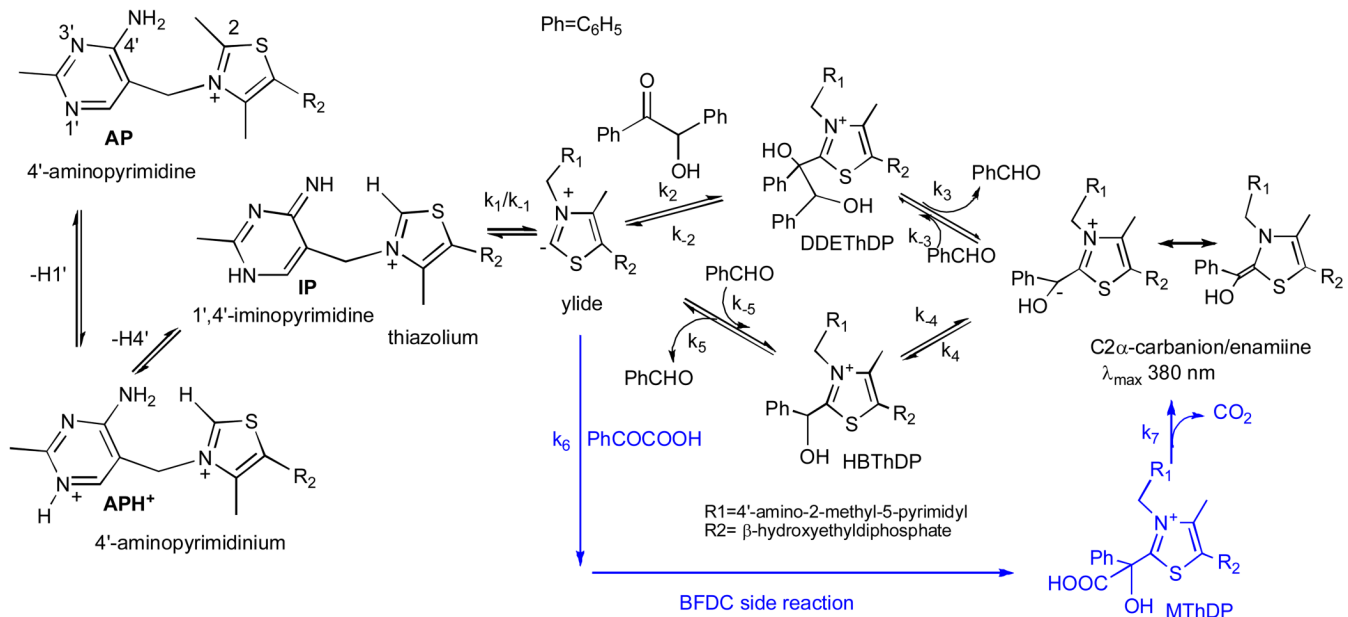
Near-UV CD spectra of wild type BAL and its H29A and W163A active center variants. (A) The comparison of the near-UV CD spectra of wild-type BAL and its H29A and W163A variants (each at concentration of 2.0 mg/ml, concentration of active centers = 33.9 μ M) recorded in 50 mM Tris-HCl (pH 8.0), containing 1 mM MgSO₄ and 0.20 mM ThDP. (B) Near-UV CD spectra of W163A BAL recorded in the absence and in the presence of 0.10–0.50 mM ThDP. Inset shows the dependence of the CD at 326 nm on the ratio of [ThDP]/[W163A BAL] (μ M/ μ M).

**Figure 9.**

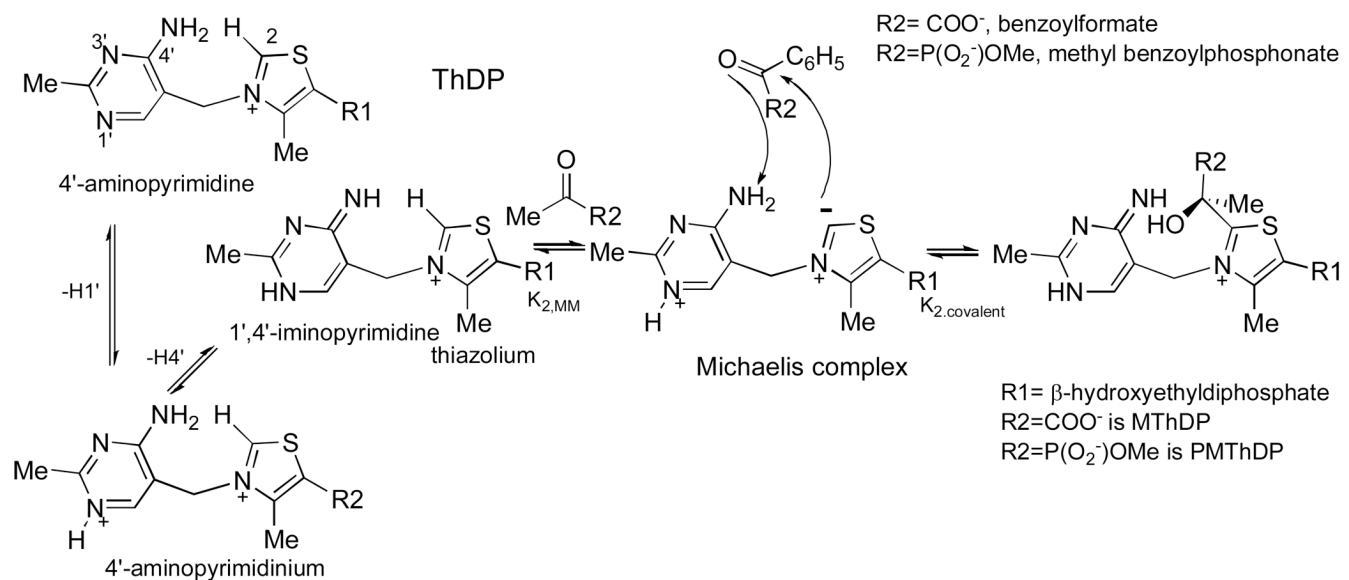
Near-UV CD spectra of H29A BAL titrated by MBP. The H29A BAL (2 mg/ml, concentration of active centers = 33.9 μM) in 50 mM Tris-HCl (pH 8.0) was titrated by 1–200 mM MBP. Inset shows the dependence of the amplitude of the CD band at 314 nm on concentration of MBP. The CD at 314 nm was obtained by the subtraction of the CD at 314 nm in the absence of MBP.

**Figure 10.**

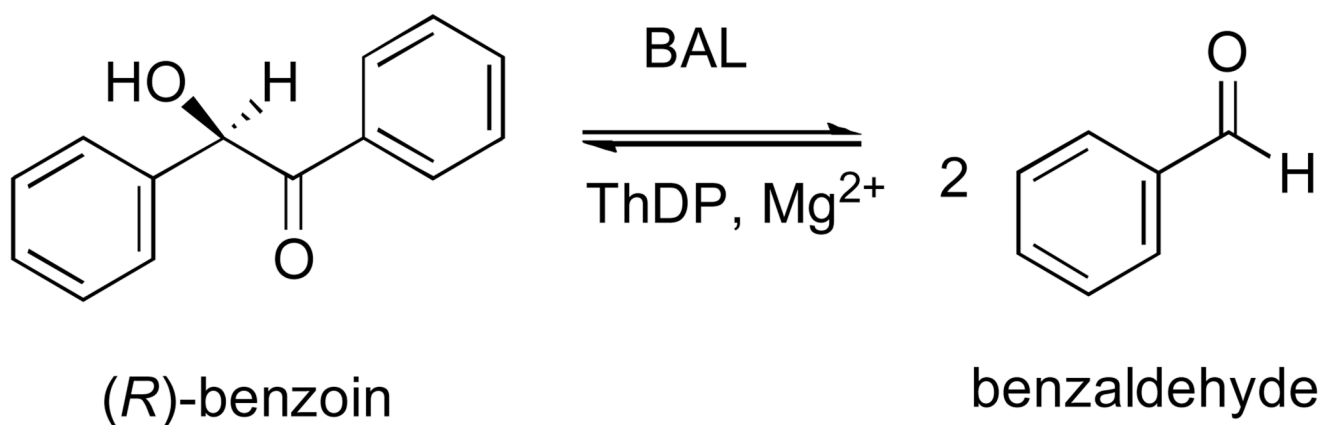
A view of the active site cleft showing the importance of Trp163 and His29 (green) in making up the active site. In addition, the relative disposition of the Trp163 and His29 sidechains may represent a geometry consistent with an energetically favorable stacking interaction. For clarity, the MBP phosphonate methyl group is not shown.

**Scheme 1.**

Proposed mechanism of reversible benzoin condensation in BAL along with the benzoylformate decarboxylase in blue.



Scheme 2.
Mechanism of formation of MThDP and PMThDP.



Equation 1.

The reaction catalyzed by benzaldehyde lyase (BAL).

Crystallographic data and model statistics

Table 1**Table 1: Data, model and crystallographic statistics for BAL structure with MBP**

PDB ID	3D7K
Beamline	APS, BioCARS, 19-ID
Wavelength (Å)	0.97934
Space group	P3 ₂ 1
Unit cell	a = b = 152 Å, c = 98 Å
Resolution limits	46.0 – 2.49 (2.59 – 2.49)
Total reflections	375040
Unique reflections	43108
Completeness % (last shell)	93.7 (79.3)
Redundancy (last shell)	8.7 (3.9)
I/σ	14.4 (1.4)
R_{merge}	0.14 (0.67)
Unit cell contents	
Molecules/ASU	2
Solvent content (%)	55.3
Refinement statistics	
Resolution range (Å)	46.0 – 2.49
R _{work} (%)	19.5
R _{free} (%)	24.9
Number of residues	1110
Number of waters	186
Average B factor (Å²)	42
RMSD	
Bond lengths (Å)	0.02
Bond angles (°)	2.3
Ramachandran analysis	
Most favored (%)	86.4
Allowed (%)	13.1
Disordered regions	
	A265–268
	A290–291
	A367–369
	A553–555
	B265–266

* Values in parentheses are for the highest resolution shell unless otherwise indicated.